INSTITUTE OF PHYSICS PUBLISHING JOURNAL OF PHYSICS: CONDENSED MATTER

J. Phys.: Condens. Matter **16** (2004) S2287–S2297 PII: S0953-8984(04)76242-6

Tunable magnetic properties of cluster assembled films grown from low temperature co-depositions

I Chado[1], J P Bucher[1], D Kechrakos[2] and K N Trohidou[2]

[1] Institut de Physique et Chimie des Matériaux, UMR 7504, Université Louis Pasteur, 23 rue du Loess, F-67037 Strasbourg Cedex, France
[2] Institute of Materials Science, NCSR 'Demokritos', 15310 Athens, Greece

Received 26 November 2003
Published 21 May 2004
Online at stacks.iop.org/JPhysCM/16/S2287
DOI: 10.1088/0953-8984/16/22/031

Abstract

Cluster assembled films are obtained by ultrahigh vacuum deposition of Co and Au vapour at low substrate temperature ($T = 30$ K). An intimate mixing of Co and Au clusters, about 20 atoms in size, is obtained after annealing to higher temperatures. In order to test the interaction between magnetic particles, controlled segregation and growth by coalescence of larger Co aggregates is achieved by further annealing. Structural as well as magnetic properties are studied *in situ* by means of variable temperature STM, LEED and MOKE. The $Co_{70}Au_{30}$ system only becomes ferromagnetic after a mild annealing to 150 K. The real time dynamic evolution of the magnetic properties is then observed *in situ* over minutes due to demixing and structural rearrangements. The superparamagnetic to ferromagnetic transition subsequent to a temperature increase are well described by Monte Carlo simulations of the phase separation and the hysteresis evolution that include exchange and dipolar interactions.

(Some figures in this article are in colour only in the electronic version)

1. Introduction

Cluster assembled materials and thin films of clusters belong to the group of nanostructured materials [1], which are attracting lots of attention, in particular for applications in magnetism, transport and optics. Among the preparation techniques the ones using cluster beam synthesis are particularly powerful since they allow good control of cluster sizes [2, 3, 5]. As far as magnetic properties are concerned, systems such as preformed Co [4] and Fe [5] clusters from a gas aggregation source have been co-deposited with Ag vapour from a Knudsen cell. These nanostructured materials have been studied for their magnetic and in particular their magnetotransport properties (GMR). The advantage of this approach is to allow an easy comparison with theoretical calculations due to the good control of cluster sizes and concentrations. Depending on the volume concentration and temperature, different regimes have been disentangled, such as single-particle blocking, collective blocking and interacting

superparamagnetism [5]. In this work we present an alternative approach based on co-deposition of metal vapour onto a substrate held at low temperature. We found that tiny clusters (a few atoms in size) spontaneously form when a sample grown at 30 K is subjected to annealing. This is a result of the high supersaturation and the small diffusion mean free path of atoms induced upon low temperature deposition. The advantage of this technique is that no cluster beam source is necessary. Furthermore, the low temperature deposition is a powerful way to force originally immiscible systems to form an alloy. In order to measure the efficiency of this technique, we choose the Co–Au system for its strong tendency to segregate [6].

Contrary to the case for bulk alloy materials, where diffusion is activated over high barriers, the enhanced surface diffusion in thin films readily allows the tuning of properties over large ranges of parameters. The magnetic behaviour is then dictated not only by the anisotropy of individual clusters but also by the interaction at various length scales through exchange and dipolar interactions. Annealing the cluster film to higher temperatures permits a fine tuning of the critical temperature T_c above which the film has a transition from ferromagnetism to paramagnetism. T_c can be adjusted from 200 K all the way up to 500 K. The same technique allows one to vary the coercive field over two orders of magnitude, from a few Oe up to 500 Oe. We found that it is necessary to keep the cluster film as thin as possible. The segregation is readily activated in samples with 2–5 ML of Co–Au but is hardly activated, if at all, in the 20 ML films. The cluster assembled films can be studied directly in the ultrahigh vacuum (UHV) vessel, after preparation, for their magnetic and structural properties.

2. Experimental details

The measurements have been performed by means of a variable temperature STM (30–600 K), in a UHV chamber with LEED and Auger facilities. Simultaneously, the magnetic properties of the cluster assembled film are followed *in situ* by means of magneto-optic Kerr effect (MOKE) measurements. The sample is permanently kept in contact with the cold finger of the cryostat; therefore all treatments and characterizations can be performed with the sample at a constant working temperature. The substrate consists of a gold single crystal previously cleaned by Ar ion bombardment and annealed at 1000 K for a few seconds. Cobalt is evaporated from a rod (99.99 purity) by electron bombardment and co-deposited with gold from an effusive cell onto the substrate at a rate of 0.025 ML min^{-1} (ML: atomic layer). During this operation, the substrate is kept at the working temperature and the pressure in the vessel remains lower than 5×10^{-10} mbar. Subsequent annealing of the supported cobalt gold deposit is done by heating the sample to the desired temperature at a rate of 1 K s^{-1}.

3. Cluster assembly and the first emergence of the MOKE signal

All the measurements have been performed on Co–Au deposits grown at a substrate temperature of $T = 30$ K. Variable temperature STM data show that clusters are already forming at a substrate temperature of 70 K. There is only a slight evolution in the topography between 70 and 160 K. Figure 1, taken at 160 K, shows a high density of small clusters, about 20 atoms in size. This comes about because the density of islands obtained in the kinetic regime is known to increase dramatically at low substrate temperatures according to the following law [7]: $N \propto R^{1/3} \exp(E_D/3kT)$, where R is the deposition rate and E_D is the diffusion barrier for an atom. As an example, taking $E_D = 0.12$ eV the saturation density of islands at 30 K is found to be $N(30\ \mathrm{K}) \approx 10^{16}$ clusters cm^{-2}. For comparison, the room temperature value is $N(300\ \mathrm{K}) \approx 10^{12}$ clusters cm^{-2}. Subsequent annealing may alter these values.

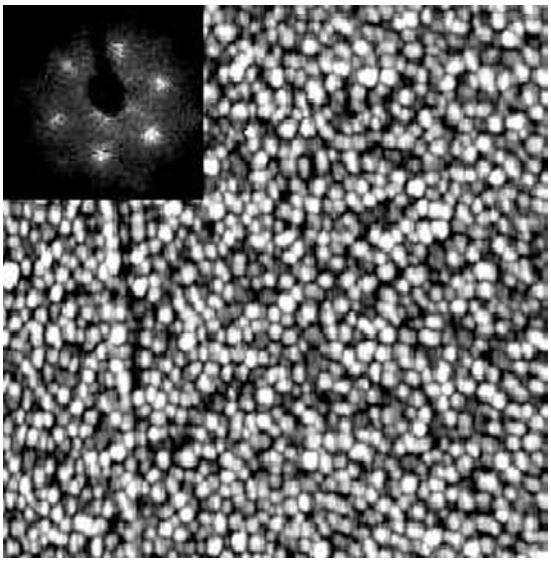

Figure 1. An STM image (100 nm × 100 nm) of 3.5 ML $Co_{70}Au_{30}$ grown on Au(111) at 30 K recorded at 160 K. Inset: the corresponding LEED diagram.

The low temperature deposit is not pseudomorphic with the crystalline substrate as revealed by the absence of a LEED diagram. As-deposited Co_xAu_{x-1} films at 30 K do not show any magnetic signal in the MOKE experiments. In the following we will focus on a Co concentration of 70% and an equivalent thickness of 3.5 ML. No magnetic signal is measured for annealing up to 140 K even after several hours of waiting time. A magnetic signal appears slowly in the polar configuration of the MOKE at $T_a = 150$ K; the signal needs about 120 min to stabilize into a nice rectangular hysteresis loop with a coercive field of 60 Oe (figure 2). The tiny clusters that make up the film start to merge into each other, thereby stabilizing the ferromagnetic phase. At a given concentration, the waiting time for the appearance of magnetism also depends strongly on the film thickness. For a 10 ML film, the waiting time is 330 min but it may become days for 20 ML. The fact that the diffusion is hardly activated in films above this thickness demonstrates the importance of surface induced diffusion.

The annealing induces considerable structural rearrangement. The appearance of a LEED diagram with a sixfold symmetry coincides with the onset of magnetism (inset of figure 1). This shows that there is a structural modification from an amorphous to a crystalline state above 150 K. Above 150 K the deposit adopts a well defined interface induced by the crystalline substrate. This is consistent with the appearance of an out-of-plane magnetization above 150 K and shows the importance of the role played by the Co–Au interface in this process (no in-plane component was observed at any stage of the annealing). Indeed, cobalt films on Au(111) grown at room temperature under similar conditions are known to possess perpendicular magnetization due to an interface contribution of the magnetic anisotropy [8–10]. This tendency has been confirmed also for Co alloys [11]. Auger electron spectroscopy (AES) confirms that during this annealing stage, there is no diffusion of Co into the Au substrate.

After annealing to T_a, the sample was cycled to lower temperature and back to T_a. The coercive field as a function of T now stays on the same curve below T_a to within the error bars (figure 3(a)). A similar result is obtained for the saturation magnetization (figure 3(b)).

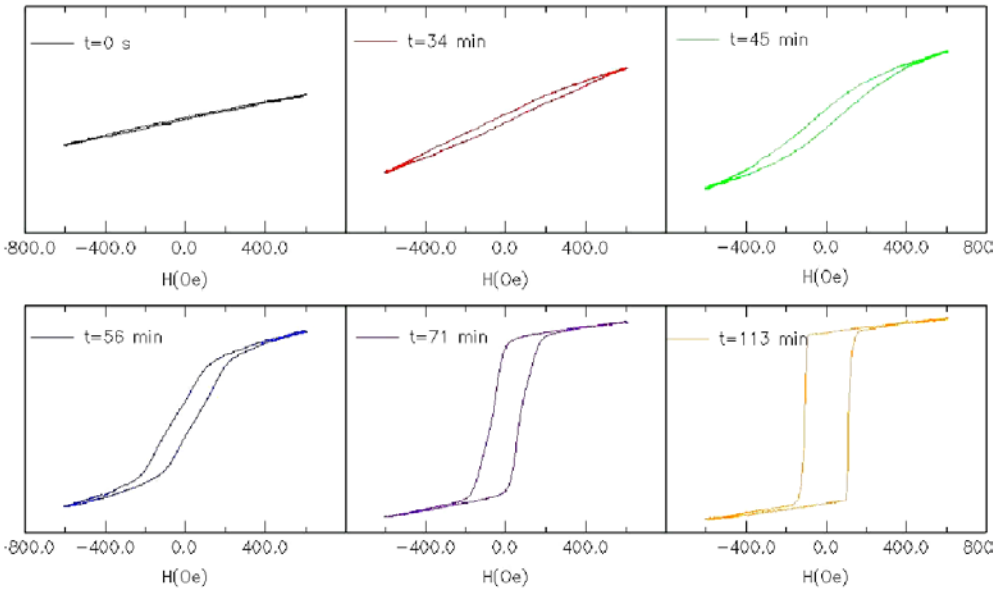

Figure 2. Polar MOKE measurements at 150 K performed under UHV. The signal of the first appearance is shown as a function of time for 3.5 ML of $Co_{70}Au_{30}$ previously grown at 30 K.

4. Dynamic evolution upon annealing

Figure 3(b) shows that the critical temperature T_c is only slightly above the annealing temperature T_a. Therefore, the evolution of the magnetic signal during a new annealing step deserves particular attention. After a sudden increase of the sample temperature above T_c, we first observe a transition to the superparamagnetic state, as expected. This manifests itself in the disappearance of the MOKE signal. As time goes on, however, the signal slowly reappears. Figure 4 shows the time evolution of the hysteresis loops after a sample, annealed at 160 K, has been subjected to a temperature step of 60 K to reach a final temperature of 220 K. In the initial stage after the temperature increase, a transition to the paramagnetic state is observed. The loop tilts strongly towards the x axis and becomes non-hysteretic. The cycle then progressively stands up as a function of time. It takes about 120 min before it is again completely rectangular.

At each new T_a, the critical temperature T_c is shifted to larger values, which clearly shows that the system evolves during annealing. It is unlikely that the effect is due to a momentary reorientation of the magnetization since no in-plane component of the magnetization was observed during the dynamic evolution. We suggest that the phenomenon is instead due to a momentarily loss of long range correlation between magnetic Co patches. The thermal excitation randomizes the orientation of magnetic moments between different spin blocks. This increase in thermal energy simultaneously induces a segregation of Au from the Co–Au alloy, resulting in the growth of larger Co patches and ultimately in bridging of the exchange interactions between Co clusters. Therefore, long range correlation appears at the new temperature and the cluster assembled system becomes ferromagnetic again.

As will be shown in the next section, the hysteresis loops (2) and (3) of figure 4 are typical for ramified Co structures with a large size distribution. Indeed, during the recovery time, the cycles are made up of a superposition of two contributions:

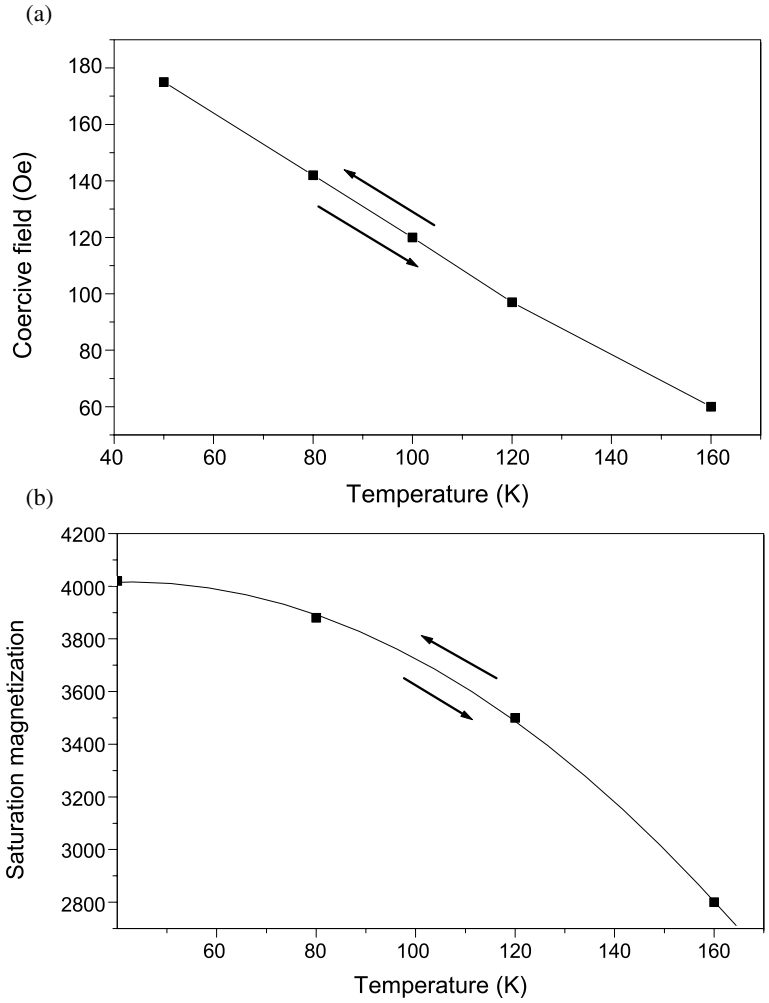

Figure 3. (a) The coercive field and (b) the saturation magnetization as a function of T for a 3.5 ML film of $Co_{70}Au_{30}$ deposited at 30 K. After a first annealing to 160 K the temperature is scanned back to 50 K and up again to 160 K (see the arrows); the two curves superimpose within experimental errors.

(i) a superparamagnetic-like contribution due to spin blocks that have randomized upon the temperature step and

(ii) a growing ferromagnetic contribution due to domains that have grown sufficiently under the thermal activation to become ferromagnetic again.

As time passes, the ferromagnetic contribution becomes more and more important because large Co domains grow at the expense of the alloy. The time evolution extends over several minutes until a new stable hysteresis loop appears with a well defined squareness. A similar phenomenon is observed for several temperature intervals 160–220, 220–300, 300–360 and 360–400 K. An annealing in steps of 10 K above 160 K leads only to a small inclination of the cycle while a step of 60 K causes the disappearance of the cycle for a few seconds. The

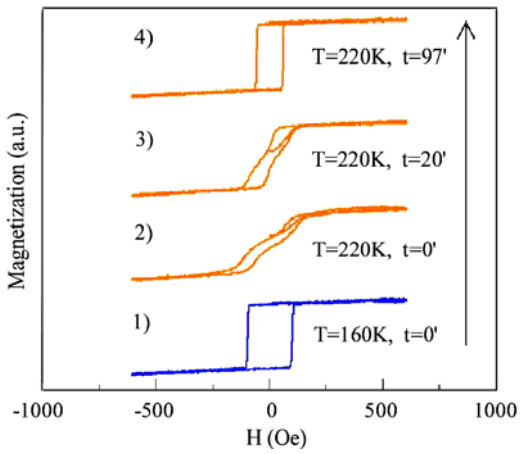

Figure 4. Real time magnetic evolution (over 97 min) of a 5 ML cluster alloy film $Co_{70}Au_{30}$ deposited at 30 K upon a temperature step from 160 to 220 K. The uncapped deposit is measured in UHV.

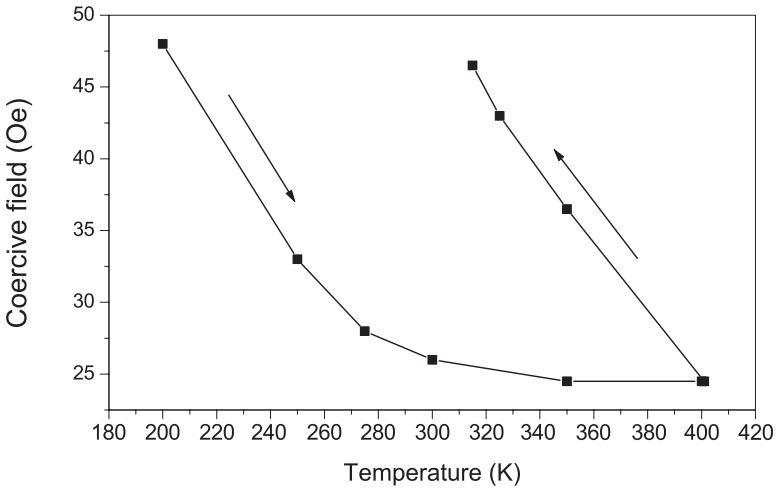

Figure 5. The variation of the coercive field upon annealing the 5 ML $Co_{70}Au_{30}$ sample up to 400 K. Lower curve: increasing temperature; upper curve: decreasing temperature below 400 K.

recovery time depends on the absolute value of the temperature. A step of 60 K will necessitate several tens of minutes of recovery at 220 K while it will take only seconds at 360 K.

From the above results it can be anticipated that thermal annealing of ultrathin cluster films can be used to carefully tune the magnetic properties. As an example, figure 5 shows how the annealing to a temperature of 400 K leads to a stable reproducible characteristic of H_c below this temperature. In other words, after a first annealing to 400 K, scanning the temperature back and forth between 320 and 400 K will lead to well defined reproducible values of H_c on the upper descending curve.

The STM pictures of figure 6 show the effect of annealing on the topography. While at 300 K the deposit shows a ramified structure, the annealing above 450 K seems to smooth the cluster film. AES measurements, however, show no evidence for phase separation in the

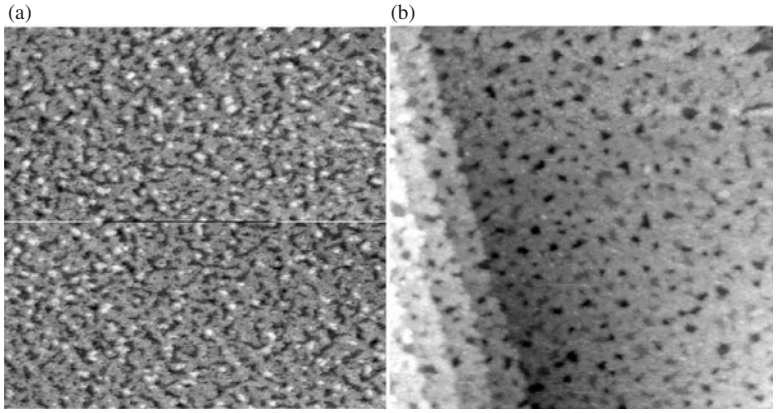

Figure 6. STM images (100 nm × 100 nm), recorded at 300 K before (a) and after (b) annealing at 495 K for 3.5 ML of $Co_{70}Au_{30}$ deposited at 30 K. Holes in the films are clearly visible. It is the presence of these vacancies that allows the segregation of Au and Co.

z direction below 450 K, in good agreement with previous measurements on the Co/Au(111) system where it has been observed that Au only goes on top of Co for annealing temperatures above 500 K [12]. It remains hard to get information on the lateral distribution of Co and Au within the film. Nevertheless, figure 6 provides prime information on the existence of vacancies in cluster assembled films. Their role in assisting domain growth is well identified [13]. Figure 6 shows that the small vacancies diffuse to form macrovacancies as is obvious when going from figures 6(a) ($T_a = 300$ K) to (b) ($T_a = 495$ K). Large holes can be seen in figure 6(b), the deepest of which are 4 ML deep. The total amount of surface vacancies is 20–25% of the film volume as estimated from the STM images by means of the Khoros software development system [14].

5. Segregation driven magnetic properties

In order to get a better insight into the segregation mechanism, we have performed Monte Carlo simulations on the phase separation of a binary alloy. The goal of the simulation is to study the tendency of the Au–Co solution to demix at a given temperature and correlate the alloy structure with the magnetic properties. The delay in the appearance of a ferromagnetic phase with increasing thickness of the deposit provides strong support for a surface induced diffusion mechanism for the Co clusters. Therefore, we believe a 2D model captures the essential features of the structural evolution of the deposited film. In our model for the phase separation we consider a binary alloy A_xB_y with a certain concentration of vacancies ($c_V = 1-x-y$) [15] on a two-dimensional triangular lattice. Repulsive pair interactions between nearest neighbour AB pairs are assumed. The Hamiltonian of the alloy is

$$H = \sum_{\langle i,j \rangle} (C_i^A C_j^A \phi^{AA} + C_i^A C_j^B \phi^{AB} + C_i^B C_j^B \phi^{BB}) \tag{1}$$

where $C_i^X = 1$ (0) if an atom X exists (does not exist) in site i and $\phi^{XX'}$ is the pair potential between atoms X and X′ that lie in nearest neighbour sites. The Hamiltonian of the binary alloy with vacancies can be transformed to an Ising Hamiltonian with spin $S = 1$:

$$H = -j_a \sum_{\langle i,j \rangle} S_i S_j + H_0 \tag{2}$$

where $J_a = \frac{1}{2}\{\phi^{AB} - \frac{1}{2}(\phi^{AA} + \phi^{BB})\}$ and H_0 is a constant. The three possible values of the spin $S_i = +1, 0, -1$ correspond to the site i being occupied by an atom A, a vacancy or an atom B, respectively. The dynamics associated with this model assumes a vacancy mechanism [13] with different jump rates (Γ_A, Γ_B) for the atoms A and B.

We have performed simulations on a 50×50 triangular lattice with periodic boundaries. For the alloy parameters we have taken $\phi^{CoCo} = -0.0837$ eV/atom, $\phi^{AuAu} = -0.0212$ eV/atom and $\phi^{CoAu} = -0.0276$ eV/atom as obtained from simple calculations[3]. The simulation is initiated from a homogeneous $Co_{70}Au_{30}$ system containing an approximate vacancy concentration $c_V \sim 25\%$ as obtained from the experiment (see above). The final results, however, do not depend critically on the vacancy concentration.

Each Co site in the simulation cell corresponds to a Co cluster in the sample. This approximation implies that the cluster–cluster interaction potentials in equation (2) should, in principle, be rescaled appropriately. That is, they should be multiplied by a factor approximately equal to the number of nearest neighbour bonds that couple two clusters. However, the as-deposited clusters are small (10–20 atoms); therefore the bridging bonds are very few and the scaling factor is approximately equal to unity. This assumption renders legitimate the use of atomic scale parameters in our model for phase separation. Snapshots of the evolution of the domains in a typical sample are shown in figure 7, where the growth of the Co domains with annealing 'time' (measured in Monte Carlo steps per spin) is demonstrated. The vacancies tend to aggregate in the interface between Co-rich and Au-rich regions, thus reducing the average size of the Co islands. We note that introduction of different rates of jumping between Co and Au, assumed proportional to their atomic masses ($\Gamma_{Au}/\Gamma_{Co} \sim 0.5$), slows the phase separation only slightly and does not introduce any qualitative differences in the final morphology of the system. We have therefore considered $\Gamma_A = \Gamma_B$.

The magnetic properties of the annealed sample are modelled by a classical Heisenberg Hamiltonian with nearest neighbour exchange interactions (J), long range dipolar interactions (g) and perpendicular anisotropy (k). The magnetic Hamiltonian is

$$H = -J \sum_{\langle i,j \rangle} \hat{S}_i \cdot \hat{S}_j + g \sum_{i,j} \frac{\hat{S}_i \cdot \hat{S}_j - 3(\hat{S}_i \cdot \hat{r}_{ij})(\hat{S}_j \cdot \hat{r}_{ij})}{r_{ij}^3} - k \sum_i S_{iZ}^2 - h \sum_i S_{iZ} \tag{3}$$

where $\langle \cdots \rangle$ indicate nearest neighbours and the hats indicate unit vectors. The last term on the right-hand side of equation (4) is the Zeeman energy due to the applied field (h). The value of the exchange energy is estimated from the wall energy as $J = 300$ K [17] while the dipolar energy between nearest neighbours is calculated to be of the order of $g = 1.5$ K.[4] Finally, the anisotropy energy is taken to be $k = 90$ K so the as-deposited Co clusters are superparamagnetic at the temperature of the simulation ($T = 300$ K). We should note at this point that the temperature value used in the simulation of the hysteresis loop ($T = 300$ K) may not be equal to the real temperature at which the magnetization measurements are made. This feature of the Monte Carlo simulation is due to the lack of true spin dynamics in the simulation method, but it does not affect the trend of hysteresis loop characteristics.

Typical runs consisted of 10^4 Monte Carlo steps per spin and 10^3 initial steps were used for thermalization. The resulting hysteresis loops were averaged over ten different samples

[3] In the simplified version of the tight binding Ising model (TBMI) used in equation (2), the pair interactions are calculated from the difference in surface energies. The sum of cohesive energies is taken to be equal to the experimental value. For an example see [16].

[4] We have used the same value for g (1 K) as in a previous study on Co clusters formed on Au surfaces [10]. Given the fact that the as-deposited clusters in the present work are smaller than the clusters in [10], the value of g (1 K) is quite overestimated for the present system. However, we have run simulations with much smaller values of g (0.1 K, 0.05 K) and the results for the hysteresis loops were almost unchanged. The role of dipolar interactions is of secondary importance for our samples, where strong exchange coupling and perpendicular anisotropy dominate.

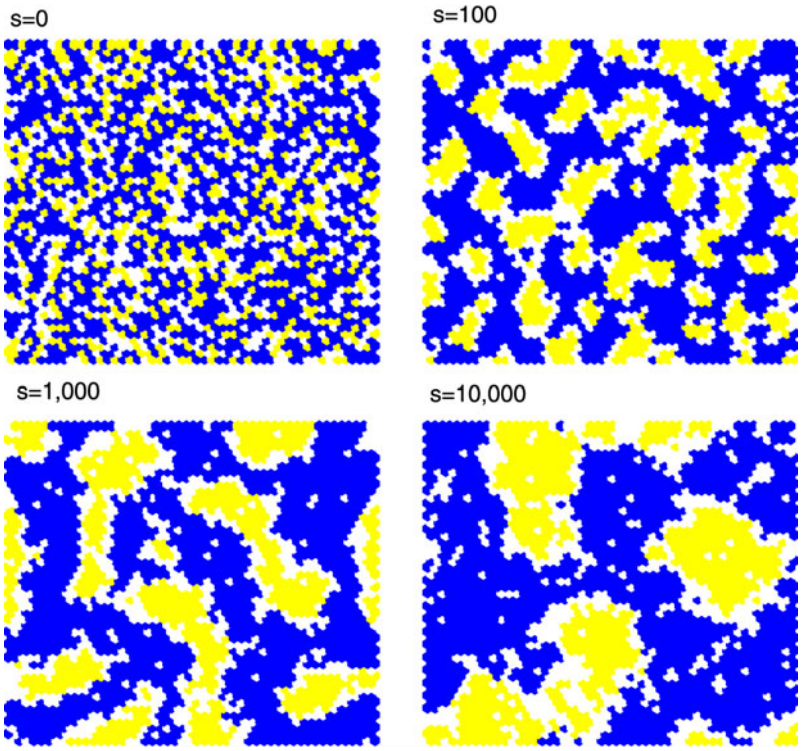

Figure 7. Segregation of a $Co_{70}Au_{30}$ cluster film with 25% vacancies at 150 K as a function of the Monte Carlo steps (s). Black sites correspond to Co atoms, gray sites to Au atoms and white sites to vacancies.

annealed under the same conditions (annealing temperature and 'time') in order to account for fluctuations in the size and shape of the Co domains. The evolution of the hysteresis loop during annealing is depicted in figure 8, where a transition from a superparamagnetic sample, exhibiting no hysteresis, to a ferromagnetic film with an almost square loop is demonstrated.

In figure 9, we have plotted the simulated evolution of the remanence and the coercivity of the $Co_{70}Au_{30}$ film together with the experimental findings for comparison. The qualitative features of the experimental measurements are satisfactorily reproduced. That is, the remanence assumes very small values at the early stages of the annealing process, as the small Co clusters are superparamagnetic. As soon as the size of the Co domains exceeds the superparamagnetic limit, which in our model is proportional to the domain area, a rapid increase of the magnetization appears that is characteristic of the ferromagnetic behaviour. A similar trend is observed in the evolution of the coercive field.

In conclusion, co-deposition of Co and Au in UHV at low substrate temperature followed by annealing leads to cluster assembled films. The immiscibility of the two components and the high mobility of atoms in ultrathin films of $Co_{70}Au_{30}$ allows one to drive the segregation of Co and Au. The alloy becomes ferromagnetic after annealing the cluster film at 150 K. A stepwise increase of the annealing temperature reveals a transition to the superparamagnetic state at each step before finally the segregation of Co again restores the ferromagnetic state on a timescale of minutes. The slow dynamics is well reproduced by a Monte Carlo simulation of the phase separation, as is the corresponding magnetic behaviour that is described by a classical

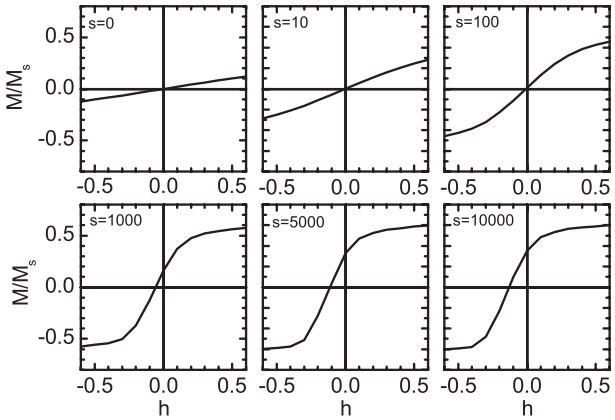

Figure 8. The time evolution of the hysteresis loop of a $Co_{70}Au_{30}$ film with 25% vacancies annealed at 150 K. Time is measured in Monte Carlo steps per site. Only the upper magnetization curve of the hysteresis loop is shown.

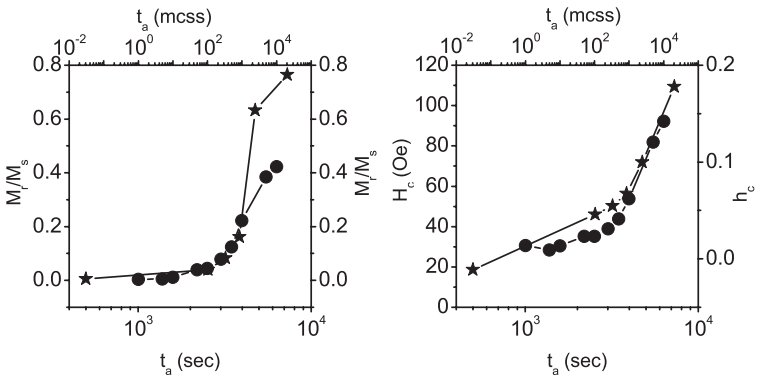

Figure 9. The time evolution of the remanence (left) and coercivity (right) of a $Co_{70}Au_{30}$ film with 25% vacancies annealed at 150 K. Stars: experimental data; circles: simulation data. The bottom and left axes in each graph correspond to experimental scales, while the top and right axes correspond to simulation scales.

Heisenberg Hamiltonian with nearest neighbour exchange interactions, dipolar interactions and perpendicular anisotropy. Finally, it is shown that tunable magnetic properties can be achieved by subjecting the cluster film to well defined annealing above room temperature. For example, the coercive field of the alloy film can be tuned from 30 Oe up to 600 Oe.

Acknowledgments

We acknowledge useful discussion with C Goyhenex on the TBMI model. This work was supported by the GROWTH project No G5RD-CT-2001-00478 from the EC.

References

[1] Gleiter H 1995 *Nanostruct. Mater.* **6** 3
[2] Perez A *et al* 1997 *J. Phys. D: Appl. Phys.* **30** 709

[3] Milani P and Iannotta S 1999 *Cluster Beam Synthesis of Nanostructured Materials* (Berlin: Springer)
[4] Parent F *et al* 1997 *Phys. Rev.* B **55** 3683
[5] Binns C, Maher M J, Pankhurst Q A, Kechrakos D and Trohidou K N 2002 *Phys. Rev.* B **66** 184413
[6] Mader S, Nowick A S and Widmer H 1967 *Acta Metall.* **15** 203
[7] Venables J, Spiller J D T and Hanbucken M 1984 *Rep. Prog. Phys.* **47** 399
[8] Chappert C *et al* 1986 *J. Magn. Magn. Mater.* **54** 795
[9] den Broeder F J A, Kuiper D, van de Mosselaer A P and Hoving W 1988 *Phys. Rev. Lett.* **60** 2769
[10] Padovani S, Chado I, Scheurer F and Bucher J P 1999 *Phys. Rev.* B **59** 11887
[11] Galanakis I, Alouani M and Dreyssé H 2000 *Phys. Rev.* B **62** 6475
[12] Speckman M, Oepen H P and Ibach H 1995 *Phys. Rev. Lett.* **75** 2035
Gentner T H, Scheurer F, Detzel T and Bucher J P 1996 *Thin Solid Films* **275** 58
[13] Komura S and Furukawa H (ed) 1988 *Dynamics of Ordering Processes in Condensed Matter* (New York: Plenum)
[14] Rasure J, Williams C, Argiro D and Sauer T 1990 *Int. J. Imaging Syst. Technol.* **2** 183
Young M, Argiro D and Kubica S 1995 *Comput. Graph.* **29** 22
[15] Yaldram K and Binder K 1991 *J. Stat. Phys.* **62** 161
[16] Treglia G, Legrand B and Ducastelle F 1988 *Europhys. Lett.* **7** 575
[17] Tannenwald P E and Weber R 1961 *Phys. Rev.* **121** 715